

Stress dependent relaxation time in large deformation

Sugeng Waluyo*

Department of Industrial Engineering, University of Jenderal Soedirman
Jl. Mayjen Sungkono Km. 5, Blater, Purbalingga, 53371, Indonesia

(Received May 18, 2016, Revised September 28, 2016, Accepted October 12, 2016)

Abstract. This work presents a new strategy to model stress dependent relaxation process in large deformation. The strategy is relied on the fact that in some particular soft materials undergoing large deformation, e.g., elastomers, rubbers and soft tissues, the relaxation time depends strongly on stress levels. To simplify the viscoelastic model, we consider that the relaxation time is the function of previous elastic deviatoric stress state experienced by materials during loading. Using the General Maxwell Model (GMM), we simulate numerically conditions with the constant and the stress dependent relaxation time for uniaxial tension and compression loading. Hence, it can be shown that the proposed model herein not only can represent different relaxation time for different stress level but also maintain the capability of the GMM to model hysteresis phenomena.

Keywords: relaxation time; large deformation; incompressible; Maxwell element; stress dependent

1. Introduction

Nowadays, advanced or smart materials based on elastomer matrix are getting their popularity. Magnetorheological elastomers (MRE) and dielectric elastomers (DE) are two common examples of them. Both materials sense magnetic and electric field by undergoing large deformation or stretch which makes their commercial application in the future are very promising as, e.g., sensors (Bahraini *et al.* 2014, Liu *et al.* 2016), actuators (Ying *et al.* 2015, Brochu and Pei 2010, Nguyen *et al.* 2014) and energy harvester (Sun *et al.* 2015, Kornbluh *et al.* 2012). Beside their large stretch capability, another important property of elastomers that must be considered for such application is relaxation time induced by viscous effects (e.g., see Kramarenko *et al.* 2015). From material design aspects, a mathematical modeling for such effect is extremely important to predict time dependent behavior either in short or long period of loading. However, since the coupled analysis for inter-relation between elastic-electric and elastic-magnetic energy are also considerably complex (Dorfmann and Ogden 2006, Itskov and Khiêm 2014, Miehe *et al.* 2015), a simple but reliable viscoelastic model to account for the viscous effect is necessary.

The large deformation viscoelasticity can be considered as the extended versions of the linear or the small strain viscoelasticity (e.g., Reese and Govindjee 1998, Simo 1987 and Holzapfel 1996), although it is not a general case. The extended versions usually use so called the General Maxwell Model (GMM) with constant relaxation time which omits the influence of stress levels to the characteristic of relaxation processes. The influence of

external factors has been formulated for examples in Bergström and Boyce (2001) by using strain rate as an exponential function of deviatoric stress norm and Tscharnuter and Muliana (2013) by introducing time-shift factor. Both models have been used to model rubber, soft tissue and general elastomeric materials only. Recently, Bortot *et al.* (2016) use the deformation gradient multiplicative split similar to Bergström and Boyce (2001) to model viscoelasticity in dielectric elastomers.

If we consider relaxation time as a material constant in the GMM, it means that for different level of stress and strain the corresponding relaxation curve yields similar relaxation behaviors. In fact, the actual tests on MRE and DE have confirmed different relaxation behavior for different level of stress and deformation (see Sahu and Patra 2016, Kramarenko *et al.* 2015). Meanwhile, to the best of our knowledge, none of the existing viscoelastic models involving large deformation above have been formulated to consider directly relaxation time as a non-constant parameter.

Therefore, we propose here a new strategy to modify relaxation time as stress dependent variable in the large deformation viscoelastic model. Another variables such as temperature is also possible to be considered but we omit it at the moment for simplicity. However, our strategy in principle can be implemented for temperature dependent relaxation time as well. Our idea is much inspired by the fact that the stress history previously experienced by material is widely known to contribute to current viscoelastic responses. To account for the fact, a convolution integral dedicated to solve differential equation for time dependent stretch evolution is normally used. In order to solve numerically the integral, we can use the time integration scheme with second order accuracy proposed by Herrmann and Peterson (1968), Taylor *et al.* (1970) and modified by Simo (1987). Meanwhile, the combination of such numerical integration with the proposed model need

*Corresponding author
E-mail: sugeng.waluyo@unsoed.ac.id

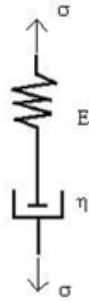


Fig. 1 The rheological model with the single Maxwell element

appropriate assumptions as follows. As our work relied on the GMM, we can simply modify the relaxation time by considering elastic stress from the corresponding branch only. The advantage of the simplification is that one can use as many as branches in the GMM to phenomenologically represent real behavior of viscoelastic materials. However, that may not be practically easy for implementation due to problem with fitting processes to determine material constants.

Furthermore, we apply here for numerical simulation a special condition regarding incompressibility constraint for isotropic viscoelastic materials under uniaxial tension and compression. In order to focus more to show the performance of our proposed model, we use simply the Neo-Hookean hyperelastic model. Although the uniaxial tension and compression are only special case of deformation, many experiments in fact are commonly done under such loadings. By taking advantage from the original properties of the GMM, our proposed strategy also can be implemented for any strain energy density function.

This paper consists of five sections including this section. In Section 2 the theoretical basis of relaxation time from the Maxwell rheological element is studied briefly. The next section shows the strategy to incorporate the stress dependent relaxation time in the stresses equilibrium state. Furthermore, we show the performance of the proposed strategy using the numerical simulation in Section 4. Finally, Section 5 outlines reviews on the performance of the proposed model.

2. Relaxation time in viscoelastic materials

In linear viscoelastic, we can derive the mathematical model of relaxation time from simple rheological model namely the Maxwell element as shown in Fig. 1. The element has parameters E and η denoting the stiffness of spring and viscosity of dashpot, respectively. The total strain rate acts on the element is the sum of strain rate from the spring $\dot{\epsilon}_E$ and the dashpot $\dot{\epsilon}_\eta$ as

$$\dot{\epsilon} = \dot{\epsilon}_E + \dot{\epsilon}_\eta \quad (1)$$

with the corresponding total stress determined by $\sigma = \sigma_e + \sigma_\eta$. In term of stress at the spring E , Eq. (1) can be expressed as

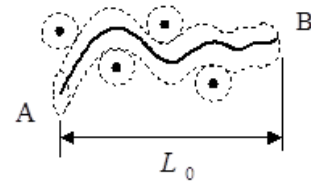


Fig. 2 The single chain (full line) inside a virtual tube (dash line), surrounded by its perpendicular chain neighbors (dot). The length of the chain at reference configuration L_0 is measured B-to-A

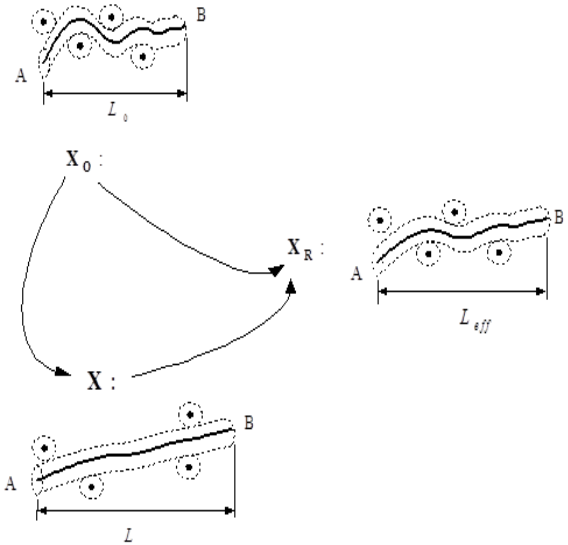


Fig. 3 The time dependent mechanisms of the chain deformation which contributes to material relaxation behaviors. The effective length of chain is measured as $L_{eff} = L - L_0$ with L as the length of chain just immediately after loading

$$E\dot{\epsilon} = \dot{\sigma} + \frac{\sigma}{\tau} \quad (2)$$

Using Eq. (2), the relaxation time is defined as the ratio between viscosity and elastic moduli, i.e., $\tau = \eta/E$, with its unit in time, e.g., second. The relaxation time is usually prescribed as a material constant in linear viscoelastic model, i.e., by assuming constant E and η in this case. However, in large deformation, such assumption is no longer appropriate since elastic moduli in hyperelastic material is widely known to be non-constant. Relied on that fact, it is more convenient if we can find alternative model to account the influence of stretch and stress state into relaxation time. Although viscosity depends strongly with temperature, we assume here that all deformation processes in this work are cold enough, i.e. no significant internal heat generated by friction.

Meanwhile, we consider the large deformation viscoelastic model proposed by Bergstorm and Boyce (2001) as the starting point for this work. Their model is inspired by time dependent mechanism of light cross linked elastomers, i.e., freely-jointed chain (FJC), consisting long strand polymeric molecules. The chain is assumed located

inside a virtual tube (see Fig. 2), which is designed to model surrounding constraint chains. With this constraint, the chain is allowed to move only inside the tube. Under external deformation field in Fig. 3, the chain or the tube is moving away from its equilibrium state X_0 to the new state X . If the applied deformation is then held constant at the state X , the chain will relax to a new state namely X_R . Measuring time required for the chain to find its new equilibrium in X_R is the key to find approximation for the relaxation time of corresponding bulk material.

Following Bergström and Boyce (2001), the rate of stretch for the deformation in Fig. 3 can be represented by a power law equation

$$\dot{\bar{\lambda}} = \dot{\bar{\lambda}}_0 (\bar{\lambda} - 1)^c \left[\frac{S^{dev}}{S_0} \right]^k \quad (3)$$

where $\bar{\lambda} = \sqrt{\text{tr}\mathbf{C}/3}$ and $S^{dev} = \|\mathbf{S}^{dev}\|$ are the effective deviatoric stretch as a function of the right Cauchy deformation tensor \mathbf{C} and the Frobenius norm of deviatoric second Piola-Kirchhoff stresses \mathbf{S}^{dev} , respectively. While S_0 , C and k are material constants related to deformation and stresses, the constant $\dot{\bar{\lambda}}_0$ is introduced mainly for dimensional consistency (see Bergström and Boyce (2001) for detail).

Not surprisingly, Eq. (3) contains two important information regarding viscosity of material η as well. First, it shows that the stress and the stretch may be independent each other with respect to rate of stretch but this can happen only in their scalar values, i.e., their average or norm. Second, Eq. (3) predicts actual *viscosity* inside material without necessary tests to obtain viscosity constant normally measured in fluid. The latter is important in the context of our proposed model here since we will work mainly with an alternative definition of viscosity to replace the definition of η in (2). How to incorporate our strategy to the linear viscoelasticity modeled by the GMM will be explained in the next section.

3. Stress dependent relaxation time

To derive stress dependent relaxation time τ^* (S^{dev}) we consider one dimensional GMM in Fig. 4. The i^{th} branch with dashpot in that figure is exactly the Maxwell element mentioned before where its stress contribution can be summed as $\sigma = \sigma_e + \sum_{i=1}^{\infty} \sigma_i$.

By using contribution of strain energy density function in the i^{th} element $W_i(\varepsilon)$, Eq. (2) can be rewritten as

$$\frac{d}{dt} \left[\frac{dW_i(\varepsilon)}{d\varepsilon} \right] = \dot{\sigma}_i + E_i \dot{\varepsilon}_{\eta,i} \quad (4)$$

with $W_i(\varepsilon) = E_i \varepsilon^2 / 2$.

To extend for large deformation in the 3-D space we propose an assumption that the scalar $E_i \dot{\varepsilon}_{\mu,i}$ in (4) can be replaced by $E_i \dot{\bar{\lambda}}_i$ and works in the direction of internal driving stress. Next, we use another assumption that the

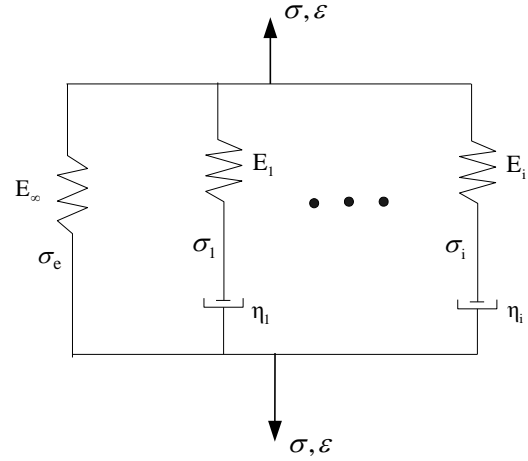


Fig. 4 The one dimensional GMM for viscoelasticity modeling with σ_e is denoted as purely elastic stress. The σ_i and η_i are the stress and the viscosity of the i^{th} Maxwell element. Long term response of this type of network depends only on the spring E_∞

driving stress itself is generated by evolution of internal stress in the i^{th} Maxwell element defined by $\mathbf{H}_i / \|\mathbf{H}_i\|$. According to Simo (1987), the internal stress \mathbf{H}_i can be defined as a non-equilibrium stress inside viscoelastic material related to a representation of different thermodynamics substate (see Truesdell and Toupin 1960). Thus, Eq. (4) becomes

$$\frac{d\mathbf{S}_i^{dev}}{dt} = \dot{\mathbf{H}}_i + E_i \dot{\bar{\lambda}}_i \frac{\mathbf{H}_i}{\|\mathbf{H}_i\|} \quad (5)$$

where $\mathbf{S}_i^{dev} = 2\alpha_i \partial W^{dev} / \partial \mathbf{C}$ is defined as the deviatoric 2nd Piola Kirchoff stress from the corresponding deviatoric part of strain energy W^{dev} . This stress makes contribution α_i to the total energy of the GMM. Meanwhile, we introduce a new definition namely $E_i = \|\mathbf{H}_i\| / \bar{\lambda}$ as the effective tangent modulus for the dashpot. With that in hand, Eq. (5) is further simplified as

$$\frac{d\mathbf{S}_i^{dev}}{dt} = \dot{\mathbf{H}}_i + \frac{\dot{\bar{\lambda}}_i}{\bar{\lambda}_i} \mathbf{H}_i \quad (6)$$

Unfortunately, solving Eq. (6) directly is difficult since we need to evaluate $\dot{\bar{\lambda}}_i(\mathbf{H}_i)$ in the *current* state of \mathbf{H}_i . Hence, motivated by relaxation processes for chain network described in Fig. 3, all the stress states can be first assumed fully elastic for each *new loading* or *unloading* step. By neglecting contribution of the viscous part due to such assumption, Eq. (6) can be solved only for $\mathbf{S}_i^{dev} = \mathbf{H}_i$ and consequently Eq. (3) becomes

$$\dot{\bar{\lambda}}_i = \dot{\bar{\lambda}}_0 (\bar{\lambda} - 1)^c \left[\frac{\|\mathbf{S}_i^{dev}\|}{S_0} \right]^k \quad (7)$$

In general S_0 , C and k can be different for each Maxwell element in the GMM but in this work we assume that all of

them are again the property of single bulk material.

With (7) in hand and $\mathbf{S}^{dev}=2\partial W^{dev}/\partial \mathbf{C}$, we are now ready to solve (6) using convolution integral over time τ as

$$\mathbf{H}_i = 2\alpha_i \int_0^t \exp\left(-\frac{(t-\tau)}{\tau_i^*}\right) \frac{d}{d\tau} [\mathbf{S}^{dev}] d\tau \quad (8)$$

where the relaxation time $\tau_i^*(s)$ in (8) is now determined by

$$\tau_i^* = \frac{\bar{\lambda}_i}{\dot{\bar{\lambda}}_0 (\bar{\lambda}_i - 1)^C \left[\frac{\|\alpha_i \bar{\mathbf{S}}^{dev}\|}{\mathbf{S}_0} \right]^k} \quad (9)$$

To evaluate (8), we perform here the numerical integration with second order accuracy developed by Herrmann and Peterson (1968), Taylor *et al.* (1970), Simo (1987) as follows

$$\mathbf{H}_{i,n+1} = \exp\left(-\frac{\Delta t}{\tau_{i,n+1}^*}\right) \mathbf{H}_{i,n} + 2\alpha_i \exp\left(-\frac{\Delta t}{2\tau_{i,n+1}^*}\right) [\mathbf{S}_{n+1}^{dev} - \mathbf{S}_n^{dev}] \quad (10)$$

with $\mathbf{H}_{i,0}=0$ and $\mathbf{S}_{i,0}=0$ for $n=0$. Hence, total stress evolution from m number of the Maxwell element can be described as

$$\mathbf{S} = \left(1 - \sum_{i=1}^m \alpha_i\right) \mathbf{S}_{n+1}^{dev} + \sum_{i=1}^m \mathbf{H}_{i,n+1} \quad (11)$$

4. Numerical experiments

In case of uniaxial incompressible loading, the deformation gradient \mathbf{F} is given by

$$\mathbf{F} = \begin{bmatrix} \lambda_1 & 0 & 0 \\ 0 & 1/\sqrt{\lambda_1} & 0 \\ 0 & 0 & 1/\sqrt{\lambda_1} \end{bmatrix} \quad (12)$$

with λ_1 representing the principle stretch for its corresponding loading direction. Using (12) we seek the solution of Eq. (11) for principle directions of the deviatoric stress \mathbf{S}^{dev} . For this purpose, we use the Neo-Hookean strain energy

$$W = (\mu/2)(\lambda_1^2 + 2\lambda_1^{-1} - 3) \quad (13)$$

to obtain the first component of \mathbf{S}^{dev} as

$$S_{11}^{dev} = \frac{1}{\lambda_1} \frac{\partial W}{\partial \lambda_1} = \mu(1 - \lambda_1^{-3}) \quad (14)$$

It is necessary to be noted here that the deviatoric stress \mathbf{S}^{dev} can be directly evaluated from (13) due to the incompressible constraint (see e.g., Simo 1987).

Consequently, the corresponding component of \mathbf{H}_i , i.e., $H_{11,i}$ is described for time $n+1$ by

$$H_{11,i,n+1} = \exp\left(-\frac{\Delta t}{\tau_i^*}\right) H_{11,i,n} +$$

$$2\alpha_i \exp\left(-\frac{\Delta t}{2\tau_i^*}\right) [S_{11,n+1}^{dev} - S_{11,n}^{dev}] \quad (15)$$

with the relaxation time $\tau_{i,n+1}^*$ is defined by

$$\tau_{i,n+1}^* = \frac{\bar{\lambda}}{\dot{\bar{\lambda}}_0 (\bar{\lambda} - 1)^C \left[\alpha_i \|S_{11,n+1}^{dev}\| / S_0 \right]^k} \quad (16)$$

with $\bar{\lambda} = \sqrt{(1/3)(\lambda_1^2 + 2/\lambda_1)}$. Thus, the total stress at the network becomes

$$S_{11} = \left(1 - \sum_{i=1}^m \alpha_i\right) S_{11,n+1}^{dev} + \sum_{i=1}^m H_{11,i,n+1} \quad (17)$$

If we see the GMM in Fig. 4, the long term response of the model in (17) is constrained by

$$E_\infty = \left(1 - \sum_{i=1}^m \alpha_i\right) S_{11,n+1}^{dev} \quad (18)$$

This work is dedicated to show the influence of stress to the behavior of stress relaxation curvature by using only *one Maxwell* element or $i=1$ in Fig. 4. In general, the relaxation time in (17) is a nonlinear function of stretch average $\bar{\lambda}$ and S_{11}^{dev} . However, since in this work our goal is only to compare results from our model to the constant relaxation time, we start by assuming only S_{11}^{dev} as the main parameters by setting $\dot{\bar{\lambda}}_0 = 1s^{-1}$, $C=0$ and $k=0.7$. The remaining parameters are determined by $\alpha_i=0.35$, $\mu=200$ MPa and $\Delta t=5$ s. Noted here that we will use the same parameters mentioned in this simulation for the next numerical simulations unless we propose other values for them.

The result in Fig. 5 by using the stress dependent relaxation time in (16) shows that the relaxation time is faster if the stress level is higher, i.e., steeper curve toward equilibrium.. Meanwhile, by using the constant relaxation

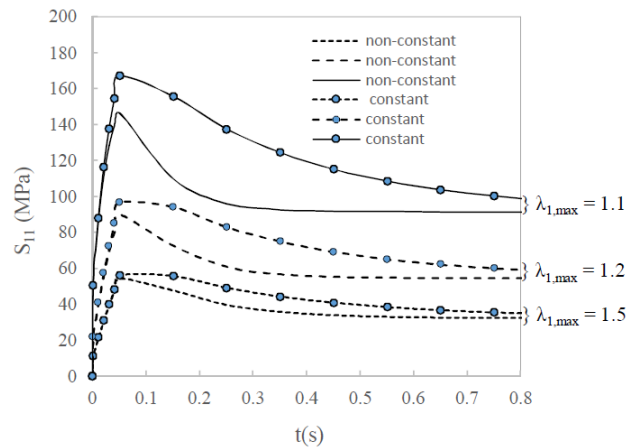


Fig. 5 Comparison of stress relaxation by using the constant and the stress dependent (non-constant) relaxation time for three different level of maximum stretches

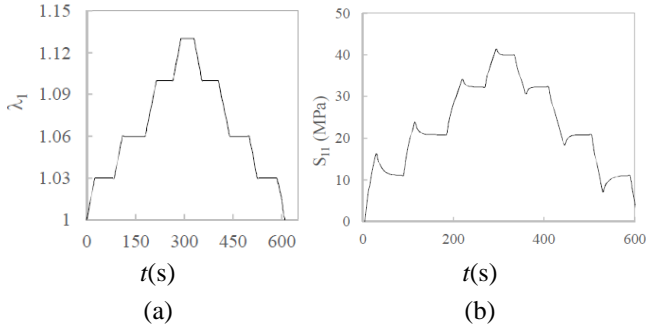


Fig. 6 Multilevel stretch history (a) to simulate the stress dependent relaxation time for loading-unloading processes (b)

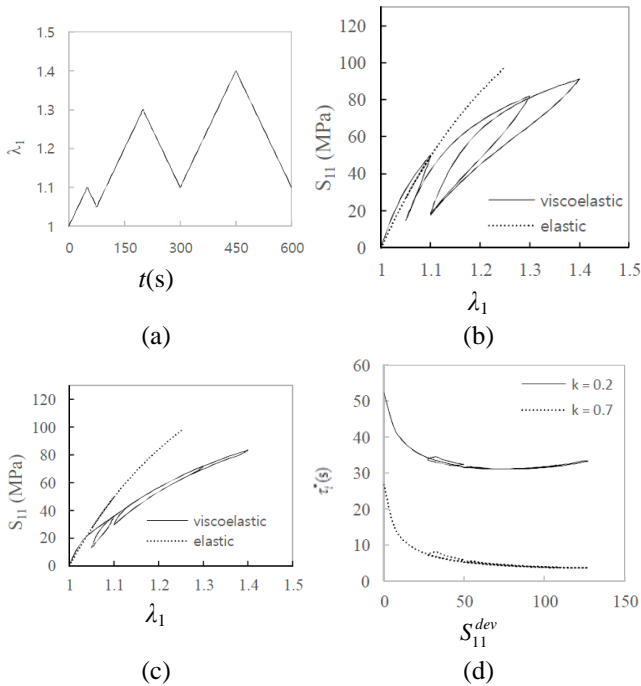


Fig. 7 The evolution of stress-stretch curve from cyclic tension loading history in (a) shows different amount of hysteresis for $k=0.2$ (b) and $k=0.7$ (c) with $\alpha_1=0.35$. Meanwhile, the corresponding evolution of α with respect to S_{11}^{dev} for both k are shown in (d). The elastic curve means the response from purely elastic stress in (14)

time we can prove also from Fig. (5) that the behavior of relaxation curves almost the same for different level of stresses. All results are obtained from the corresponding constant maximum stretches $\lambda_{1,max}=1.1$, $\lambda_{1,max}=1.2$ and $\lambda_{1,max}=1.5$ for duration $t=0.8$ s.

Moreover, it is also interesting to use relaxation time in (16) for more complex loading-unloading behavior as shown in Fig. 6(a). Using the same parameters above but with $\dot{\lambda}_0=0.01s^{-1}$, the result of simulation in Fig. 6(b) shows different behavior of relaxation for higher stress not only during loading but also unloading processes. It is also shown here that at the end of loading time, i.e., $t=600$ s, the material does not return to stress free condition but still has small value of residual stress. This phenomenon is well-

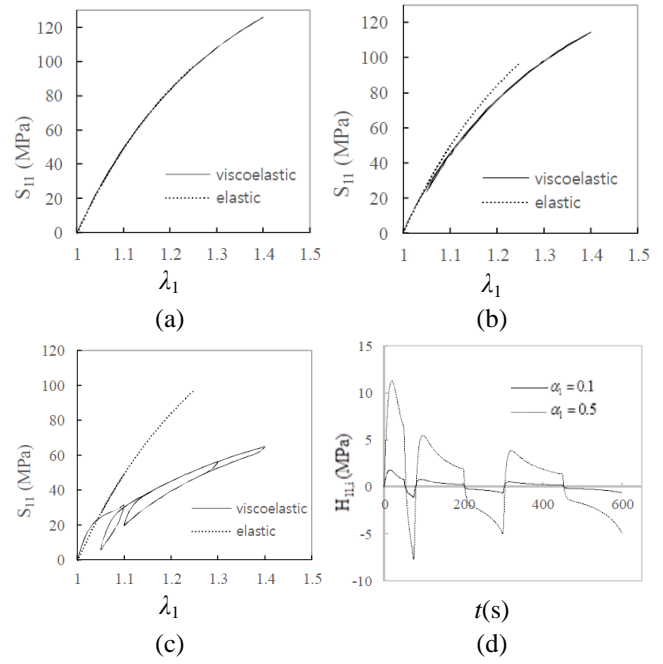


Fig. 8 The evolution of stress-stretch curve using the same loading in 7(a) with $k=0.7$ for $\alpha_1=0.01$ (a), $\alpha_1=0.1$ (b) and $\alpha_1=0.5$ (c). Meanwhile, the corresponding evolution of $H_{11,1}$ for $\alpha_1=0.1$ and $\alpha_1=0.5$ are shown in (d)

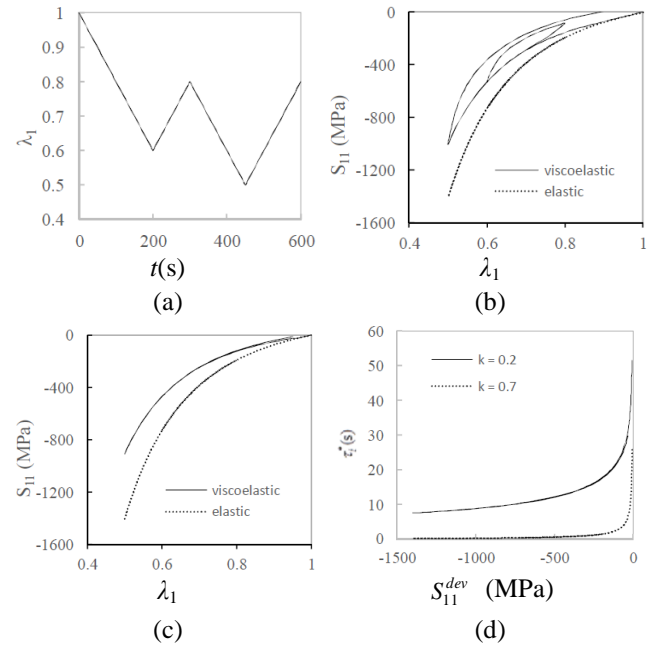


Fig. 9 The evolution of stress-stretch curve from cyclic compressive loading history in (a) shows different amount of hysteresis with $k=0.2$ (b) and $k=0.7$ (c) with $\alpha_1=0.35$. Meanwhile, the corresponding evolution of S_{11}^{dev} with respect to S_{11}^{dev} for both k are shown in (d). The elastic curve means the response from purely elastic stress in (14)

known in viscoelastic materials as temporary energy losses due to viscosity.

Furthermore, we simulate cyclic tension loading using stretch history shown in Fig. 7(a) to study important aspects

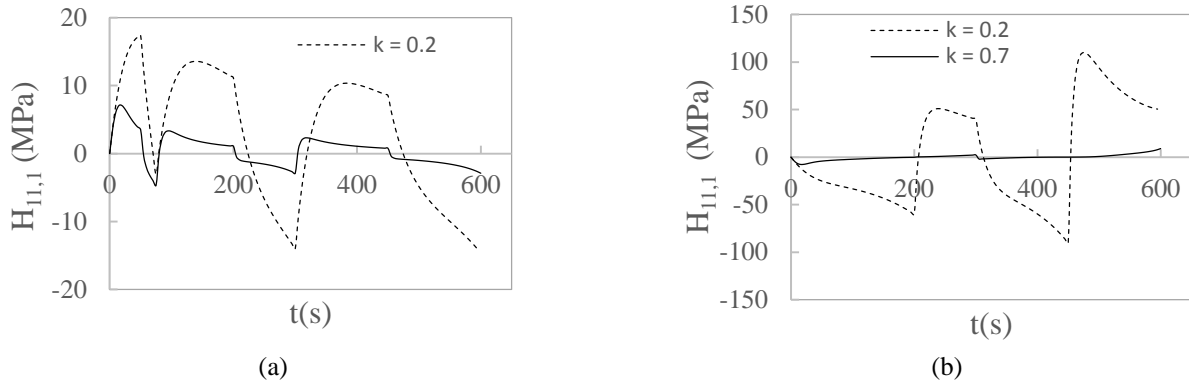


Fig. 10 The evolution of internal stress $H_{11,1}$ from cyclic tension (a) and compression (b) simulation in Figs. 7 and 9, respectively

regarding the influence of deformation rate during loading and unloading with respect to the viscoelastic material responses. By using $\alpha_1=0.35$ the values of k are varied for $k=0.2$ and $k=0.7$. The simulation results are shown in Fig. 7(b) and 7(c) where under higher influence of the stress, i.e., higher k , energy dissipation represented by the area between adjacent loading and unloading curve will be lower. The area here indicates well-known hysteresis processes where it will disappear for purely elastic deformation. The evolution of the relaxation time (16) in Fig. 7(d) shows that only the level of stress significantly influences the relaxation time but not for the previous history of loading. This conclusion comes from the result in Fig. 7(d) that the responses from cyclic loading are almost coincide at single curve for both $k=0.2$ and $k=0.7$.

Furthermore, we set another cyclic tension loading simulation in the opposite way by prescribing $k=0.7$ for $\alpha_1=0.01$, $\alpha_1=0.1$ and $\alpha_1=0.5$. Because α_1 is also related to stiffness at the infinite time, the simulation is dedicated to find contribution of the Maxwell element to hysteresis. Using the same loading as Fig. 7(a), results in Fig. 8 show behavior of the stress-stretch curves which move from completely elastic case with the long term stiffness for $\alpha_1 \rightarrow 0$ to the completely fluid with $\alpha_1 \rightarrow 1$. The relaxation time implicitly represented by the area of hysteresis is also clearly a function of stress level. Hence, our proposed relaxation time is more flexible to represent hysteresis processes in viscoelastic materials than the constant relaxation time. Additionally, we are also interested to capture the evolution of the internal stress-like variable $H_{11,1}$ as shown in Fig. 8(d). From the figure it increases rapidly until certain loading time and decreases afterwards also under loading condition. This is typical situation where the accumulation of previous internal variable plays significant role.

The extension from the numerical experiment in Fig. 7 in order to incorporate more than one Maxwell element, i.e., using $\alpha_2, \alpha_3, \dots, \alpha_\infty$, is straightforward. However, following the additive scheme shown in (17) and (18) such extension will not significantly change the hysteresis area already obtained in Figs. 7 and 8 unless the contribution from the viscous branch changes. This is because for the same $\alpha_\infty = 1 - \sum \alpha_i$ in (18) the extension will produce the same

amount of viscous response although it is now shared among each Maxwell element in the GMM. Under the extension, the contribution from each viscous branch will appear only in relaxation curves, e.g. similar curves shown in Figs. 5 and 6. We aim to study this topic using actual data from material testing in the future.

For completeness, we perform cyclic uniaxial compression simulation driven by the loading history in Fig. 9(a). The results are presented in Figs. 9(b) and 9(c) where the viscoelastic responses will approach the elastic solution for small k . However, different result from the tension simulation at $k=0.7$ are observed in Fig. 9(c) where the hysteresis area is smaller than in Fig. 7(c). This fact confirms that the viscoelastic behavior is also built by the corresponding hyperelastic model which normally gives different responses under tension and compression loading. Similar to the tension test, the evolution of τ_1^* in Fig. 9(d) shows similar trend as the tension test which is explicitly as the function of the stress level.

Finally, the evolution of $H_{11,1}$ for tension and compression loading in Fig. 7 and Fig. 9 are shown in Fig. 10. Since $H_{11,1}$ is also a function of S_{11}^{dev} through τ_1^* , we observe again that both evolution are built mainly by different behavior of the Neo-Hookean model under tension and compression loading. Meanwhile, the same situation from Fig. 8(d) is observed in Fig. 10(a) that $H_{11,1}$ in the tension simulation increases rapidly during loading but decreases after certain loading time towards a compressive state. Surprisingly, the situation occurs in the opposite way for the compression simulation as shown in Fig. 10(b). By the application of compressive loading, $H_{11,1}$ increase slowly under the compressive loading but suddenly moves to a tensile state after certain period of unloading process. This is typical situation where the accumulation of $H_{11,1}$ from the previous time n has been in a tension state and significantly influences the relaxation behavior in the current time. As a result, it still has capability to control the overall response of the material during unloading processes.

5. Conclusions

By re-definition of relaxation time in the linear GMM

model to be stress dependent parameters, different types of stress relaxation curves for different stress levels are obtained in this work. As the stress level is higher, the long term equilibrium in materials is achieved faster by using our model which does not occur in case of the relaxation time is given by constant for any stress levels. Furthermore, our model is also successfully implemented in loading-unloading scenario to produce hysteresis phenomena. The influence of stress to relaxation time appears also in the cyclic simulation with the same tendency as the stress relaxation curves previously mentioned. Finally, according to our model, for larger contribution of the single Maxwell element compared to the long term response branch, loss of energy during hysteresis is higher.

Acknowledgments

The research described in this paper was financially supported by Lembaga Pengelola Dana Pendidikan (LPDP)-Republic Indonesia.

References

- Bahraini, S.M.S., Eghtesad, M., Farid, M. and Ghavanloo, E. (2014), "Analysis of an electrically actuated fractional model of viscoelastic microbeams", *Struct. Eng. Mech.*, **52**(5), 937.
- Bergström, J.S. and Boyce, M.C. (2001), "Constitutive modeling of the time-dependent and cyclic loading of elastomers and application to soft biological tissues", *J. Mech. Mater.*, **33**(9), 523-530.
- Bortot, E., Denzer, R., Menzel, A. and Gei, M. (2016), "Analysis of viscoelastic soft dielectric elastomer generators operating in an electrical circuit", *Int. J. Solid. Struct.*, **78**, 205-215.
- Brochu, P. and Pei, Q. (2010), "Advances in dielectric elastomers for actuators and artificial muscles", *Macromol. Rapid Commun.*, **31**(1), 10-36.
- Dorfmann, A. and Ogden, R.W. (2006), "Nonlinear electroelastic deformations", *J. Elasticity*, **82**(2), 99-127.
- Herrmann, L.R. and Peterson, F.E. (1968), "A numerical procedure for viscoelastic stress analysis", *Proceedings of the Seventh Meeting of ICRPG Mechanical Behaviour Working Group*, Orlando.
- Holzappel, G.A. (1996), "On large strain viscoelasticity: continuum formulation and finite element applications to elastomeric structures", *Int. J. Numer. Meth. Eng.*, **39**, 3903-3926.
- Itskov, M. and Khiêm, V.N. (2014), "A polyconvex anisotropic free energy function for electro-and magneto-rheological elastomers", *Math. Mech. Solid.*, 1081286514555140.
- Kornbluh, R.D., Pelrine, R., Prahlad, H., Wong-Foy, A., McCoy, B., Kim, S. and Low, T. (2012), "From boots to buoys: promises and challenges of dielectric elastomer energy harvesting", *In Electroactivity in Polymeric Materials*, Springer, US.
- Kramarenko, E.Y., Chertovich, A.V., Stepanov, G.V., Semisalova, A.S., Makarova, L.A., Perov, N.S. and Khokhlov, A.R. (2015), "Magnetic and viscoelastic response of elastomers with hard magnetic filler", *Smart Mater. Struct.*, **24**(3), 035002.
- Liu, Y., Han, H., Liu, T., Yi, J., Li, Q. and Inoue, Y. (2016), "A novel tactile sensor with electromagnetic induction and its application on stick-slip interaction detection", *Sensor*, **16**(4), 430.
- Miehe, C., Vallicotti, D. and Zäh, D. (2015), "Computational structural and material stability analysis in finite electro-elastostatics of electro-active materials", *Int. J. Numer. Meth. Eng.*, **102**(10), 1605-1637.
- Nguyen, C.T., Phung, H., Nguyen, T.D., Lee, C., Kim, U., Lee, D., Moon, H., Koo, J., Nam, J. and Choi, H.R. (2014), "A small biomimetic quadruped robot driven by multistacked dielectric elastomer actuators", *Smart Mater. Struct.*, **23**(6), 065005.
- Reese, S. and Govindjee, S. (1998), "A theory of finite viscoelasticity and numerical aspects", *Int. J. Solid. Struct.*, **35**(26), 3455-3482.
- Sahu, R.K. and Patra, K. (2016), "Rate-dependent mechanical behavior of VHB 4910 elastomer", *Mech. Adv. Mater. Struct.*, **23**(2), 170-179.
- Simo, J.C. (1987), "On a fully three-dimensional finite-strain viscoelastic damage model: formulation and computational aspects", *Comput. Meth. Appl. Mech. Eng.*, **60**(2), 153-173.
- Sun, W., Jung, J. and Seok, J. (2015) "Frequency-tunable electromagnetic energy harvester using magneto-rheological elastomer", *J. Intel. Mater. Syst. Struct.*, 1045389X15590274.
- Taylor, R.L., Pister, K.S. and Goudreau, G.L. (1970), "Thermomechanical analysis of viscoelastic solids", *Int. J. Numer. Meth. Eng.*, **2**, 45-59.
- Truesdell, C. and Toupin, R. (1960), *The Classical Field Theories, Principles of Classical Mechanics and Field Theory/Prinzipien der Klassischen Mechanik und Feldtheorie*, Springer, Berlin Heidelberg.
- Tscharnuter, D. and Muliana, A. (2013), "Nonlinear response of viscoelastic polyoxymethylene (POM) at elevated temperatures", *Polymer*, **54**(3), 1208-1217.
- Ying, Z.G., Ni, Y.Q. and Duan, Y.F. (2015), "Stochastic micro-vibration response characteristics of a sandwich plate with MR visco-elastomer core and mass", *Smart Struct. Syst.*, **16**(1), 141-162.

CC